

## **Experimental and numerical analyses of the tensile strength and mixed-mode fracture behavior of sheet molding compound plates**

**DOI:10.36909/jer.15615**

Adem Avcu, Naghdali Choupani, Cem Boğa, Mirsadegh Seyedzavvar\*, Burçak Zehir

*Faculty of Engineering, Adana Alparslan Türkeş Science and Technology University, Adana, Turkey*

\* Corresponding Author: mseyedzavvar@atu.edu.tr

### **ABSTRACT**

Polymer matrix composites are the most prevalent ones among all the composite materials because they offer high specific strength to weight ratio, toughness, and ease of processing. These composites own most of their properties to the high-strength reinforcement materials as carbon, glass, and aramid fibers. The mass production method of such composites is basically the sheet molding compound (SMC) compression molding technology. However, regarding the inherent defects of SMCs, such as porosities and internal cracks, the current trend of improving their performance requires a thorough understanding of mechanical and fracture properties of such products. Therefore, in this work, the commercially available chopped glass-fiber reinforced polyester SMC has been subjected to uniaxial tensile and mixed-mode fracture experiments, along and perpendicular to the rolling direction. The results of these experiments were employed as input data in a finite element model to determine the fracture toughness ( $K_{IC}$  and  $K_{IIC}$ ) and critical strain energy release rate ( $G_{IC}$  and  $G_{IIC}$ ) of material under mixed-mode loading conditions. Overall, although the reinforcing material were in the form of strands of glass fiber, SMC specimens exhibited lower mechanical properties and fracture toughness in transverse direction as compare with that of the longitudinal (rolling) direction under all modes of loadings.

**Keywords:** SMC plate; Arcan specimen; mixed-mode fracture; fracture toughness; strain energy release rate

## INTRODUCTION

The application of plastic composites have been expanding in more areas of engineering because of their advantages over traditional ceramic composites such as high weight to strength ratio, mechanical properties, and more resistance against degradation (Aramide *et al.*, 2012, Lau *et al.*, 2018). Since the composites are made of two or more phases, they could also be formulated, in terms of filling ratios, size and type of constituents, to meet specific design requirements or acquire typical characteristics necessary for an application (Todor *et al.*, 2018). Among the fiber reinforced composites, the application of polymer matrix composites (PMCs) is prevalent in automotive industry as body panels, bumpers and so on (Çakmakkaya *et al.*, 2019). The reinforcement constituents are in the form of continuous and discontinuous fibers, or particles. The composites with continuous fibers provide the maximum stiffness and strength, however the production process is more difficult and costly. The application of discontinuous fibers leads to reduction in manufacturing cost and ease in production process at the expense of mechanical properties as compared to that of continuous fibers (Barbero, 2017). Sheet molding composite (SMC) is a ready to mold short glass fiber reinforced composite plates with a matrix usually made of epoxy, vinyl ester or polyester (Mallick, 2012).

However, the mechanical properties of SMCs are significantly influenced by the process parameters (Martulli *et al.*, 2019). The random orientation of chopped fibers with respect to the rolling direction may impose anisotropic mechanical properties in the final products. Additionally, the presence of porosities in the matrix or incomplete fusion between the fibers and the matrix have negative effects on the fracture toughness of the SMCs. Kelly *et al.* (2018) showed that the

tensile and flexural strengths of SMC increase while the elongation at break decreases with increasing weight fraction of glass fibers in a polyether ether ketone (PEEK) matrix. Martulli *et al.* (2019) showed that the orientation of the carbon fiber in the resin matrix significantly affect the material failure, whereas the local manufacturing defects had little influence. They reported that along the direction of fiber orientation, the SMCs were 27% stiffer and 66% stronger than what has been for a material of random fiber orientation. Nony-Davadie *et al.* (2019) investigated the anisotropic effects of orientation of randomly distributed carbon fiber in SMCs, containing 25.4 mm carbon bundles with weight ratio of 55% in a vinyl-ester matrix which were subjected to quasi-static and fatigue loadings. Based on the X-ray analyses and SEM observations, the authors reported that occurrence of damage mechanisms such as microcracks between and inside the fiber bundles depends on the fiber orientation in the matrix. Gupta *et al.* (2021) introduced the biodegradable banana fibers as reinforcement in the resin matrix with layout of 2-layers of fibers and 3-layers of resin. They examined the tensile and bending strengths as well as the impact resistance of the composite panels using the samples cut in standard dimensions by waterjet process. The authors reported that the enhancement in the aforementioned properties of the composite panels are dependent to the orientation of the fibers in the matrix.

Although, the introduction of SMC was a revolution in parts manufacturing for shifting away from metals, there is still a need for a thorough understanding of the fracture properties of these material as there is no specific research addressing these properties of the SMCs. The intrinsic defects that may appear in SMCs, such as porosity, microcracking and segregation between the bundles and the matrix, render the concept of strength of materials not sufficient in defining the mechanical properties of such materials. To this end, examining the behavior of materials in the event of fracture and cracking of the material provides valuable data for development of reliable

parts (Abadi *et al.*, 2019). There are many different methods to investigate the fracture toughness of material, namely compact tension specimen (CTS), double edge notched tension (DENT), center notched tension (CNT), single edge notched tension (SENT), and three-point bending (3PB) experiments mainly used for mode-I fracture. The end-notched flexure (ENF) or end loaded split (ELS) and asymmetric four-point bend (A4PB) tests are preferred for mode-II fracture experiments (Pfeiffer and Wriggers, 2012). However, for mixed-modes of fracture, unlike the conventional methods, the Arcan named sample facilitates the measurement of the fracture toughness in mixed-mode loadings using a single experiment.

Based on the literature review and to the best of the authors' knowledge, there are few studies on the behavior of SMCs under mixed-mode loadings. To this end, in this study, experiments were conducted to investigate the tensile strength and fracture toughness of SMC material in both longitudinal and transverse directions with respect to the rolling direction such material. Next, the numerical modelling of Arcan specimens were performed using Abaqus software in order to obtain the shape function (geometry correction factor) and also critical strain energy release rate of Arcan samples under mixed-mode loadings.

## **MATERIALS AND METHODS**

### **Composite material and test samples**

The SMC plates have been supplied from Milen Tech and Tetraktis Composite CO. in the form of a vinyl ester matrix reinforced by 15 mm chopped glass fibers with weight fraction of 53%. The production process of SMC is schematically shown in Figure 1. Accordingly, the resin is applied in the form of a paste to a film that passes between the rollers. The glass fibers are chopped and added to the paste that covers the film. Also, some additives, in the form of sizing material, are added to the paste to improve the binding between the fibers and the resin. Next, a second film is

applied on the constituents, and they all are squeezed between rollers until the desired thickness of the product is achieved. The pre-impregnated sheets of fibers and matrix are cut into small plates called charges that are placed between two halves of a flat mold mounted on panels of a hot-press, at temperature 140°C and pressure of 70 bar, to fully cure the resin and achieve flat panels of thickness of 5 mm.

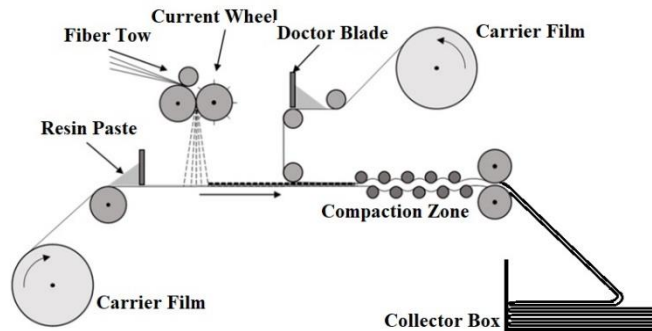


**Figure 1.** Schematic representation of production process of sheet molding compound (Kelly *et al.*, 2018).

SMC plates were cut using a high-pressure waterjet cutting machine in accordance with the dimensions of the dumbbell-shaped tensile and Arcan specimens. The cutting process and the obtained test samples are shown in Figure 2. Accordingly, the tensile test and Arcan specimens were cut in longitudinal and transverse directions of the SMC plates with respect to the rolling direction in production process. The dimensions of the dumbbell-shaped samples based on D638 ASTM standard is shown in Figure 3.

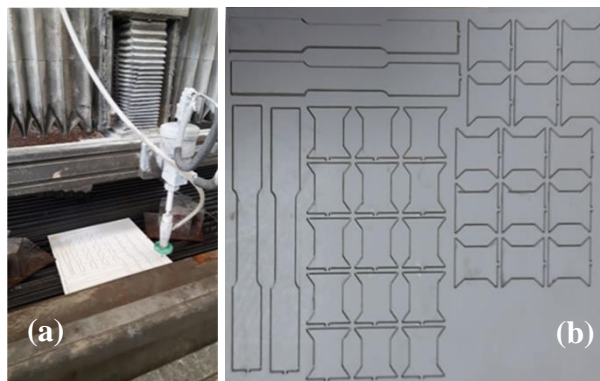


**Figure 2.** Representation of waterjet cutting process of specimens; (a) cutting process and (b) final form of the specimens.

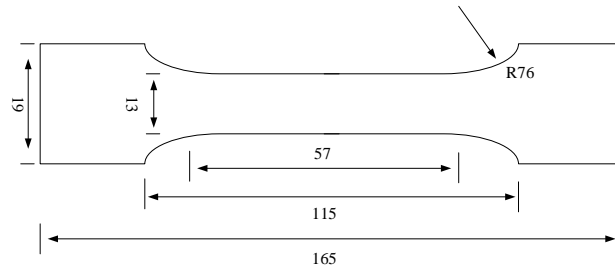


**Figure 3.** 2D representation of dumbbell-shaped tensile test specimen.

### Uniaxial tensile and mixed-mode fracture tests

The uniaxial tensile and mixed-mode fracture tests were performed using a Shimadzu tensile test machine. Three tensile tests were conducted for each longitudinal and transverse directions of the SMC plates and the mechanical properties were reported based on the average stress-strain curves. The Arcan specimen and the specially designed fixture to apply mixed-mode fracture loading using the uniaxial tensile test machine is shown in Figure 4. Accordingly, the sample thickness was 5 mm, with crack length of 10 mm and the width of 20 mm. Arcan sample was introduced to produce uniform stress state in crack-tip of specimen. It is based on the fact that transmission of shear forces between the edges of a notch produces an approximately uniform shear stress along that section (Ganesan, 2008). The configuration of Arcan fixture (Figure 4) allows the application of biaxial loadings at any combination of pure-shear to traverse tension.

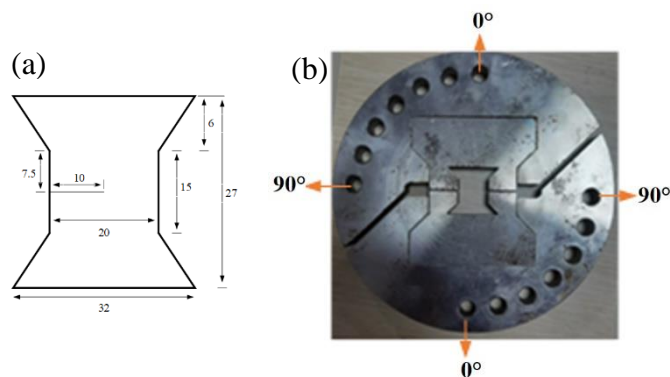


**Figure 4.** (a) Arcan specimen and (b) specially designed fixture for mixed-mode fracture experiments.

In total, 28 Arcan specimens were prepared to perform mixed-mode fracture tests, half of which were cut in longitudinal and the other half in the transverse directions of the SMC plates. Furthermore, three tests were conducted for each loading angle and the average curves have been selected as the load-displacement curve of fracture under specific loading condition. The fracture experiments at three modes of loadings, including mode-I (opening mode), mixed-mode I/II (45° loading), and mode-II (shearing mode), are shown in Figure 5. Overall, the experiments were carried out at 7 different loading angles with 3 repetitions at each loading angle.

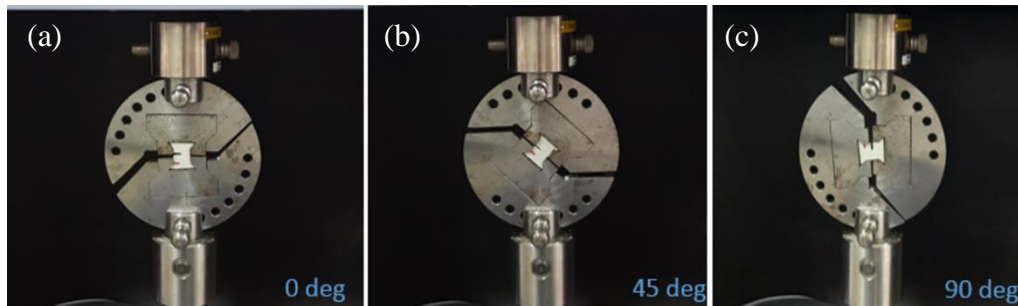


**Figure 5.** Fracture loading at; (a) mode-I, (b) mixed-mode I/II, and (c) mode-II.

### Finite element modeling of Arcan samples

A finite element model (FEM) was developed using Abaqus software to achieve the geometry correction factors of Arcan specimen. As shown in Figure 6a, the model was partitioned into the fixture and the Arcan geometries and the interaction between them was defined as hard contact. Subsequently, the AISI 4140 stainless-steel mechanical properties, presented in Table 1, and the SMC transversely isotropic properties, represented in results and discussion section, were assigned to the fixture and Arcan sections, respectively. Also, a close-up view of the Arcan sample can be seen in Figure 6b. The initial ratio of crack length to width for all samples were held as  $a/w=0.5$  and the entire specimen was modeled using eight node collapsed quadrihedral element and the mesh was refined around the crack-tip (Figure 6c). A linear elastic finite-element analysis was

performed under a plane strain condition using  $1/r^{0.5}$  stress field singularity. To this end, the elements around the crack-tip were focused on the crack-tip and the mid-side nodes were moved to a quarter point of each element side. Therefore, the smallest element size found in the crack-tip was approximately 0.25 mm (Choupani, 2008). The typical result of FEM of maximum principal strain energy distribution at the crack-tip for mode-I loading of 3000 N is represented in Figure 7.

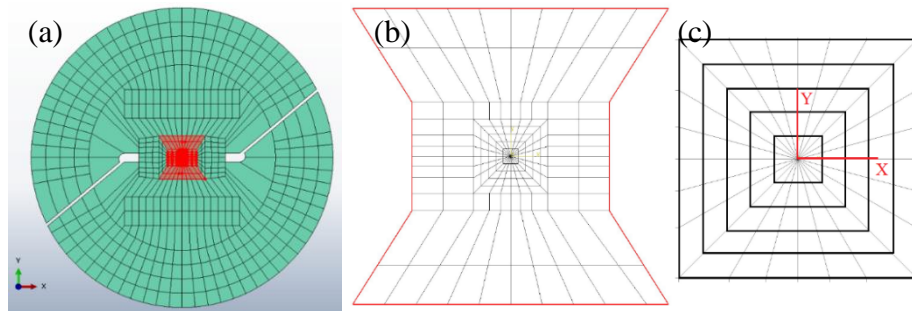


**Figure 6.** Finite element model of fracture experiment; (a) partition of the model, (b) close-up view of the Arcan sample, and (c) 5-contours at the crack-tip.

**Table 1.** Mechanical properties of AISI 4140 stainless steel (Madduru *et al.*, 2014).

Property	Value
Modulus of elasticity, E (GPa)	210
Poisson's ratio, $\nu$	0.3
Density, $\rho$ (g/cc)	7.85
Yield strength, $\sigma_y$ (MPa)	415
Ultimate strength, $\sigma_u$ (MPa)	655

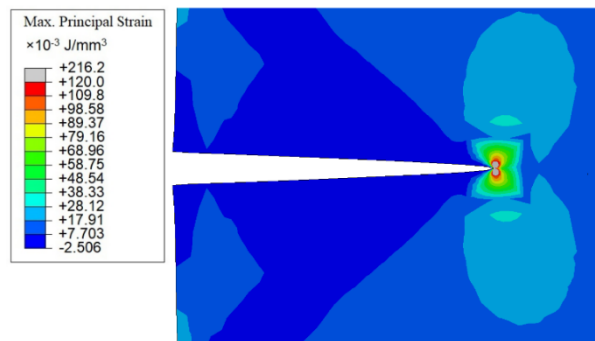


**Figure 7.** Maximum strain energy distribution at the crack-tip under mode-I loading.

The shape functions of Arcan sample have been calculated using the stress-intensity factor and the following equations. The results are given as curves in Figure 8.

$$K_I = \frac{P\sqrt{\pi a}}{wt} f_I\left(\frac{a}{w}\right) \quad (1)$$

$$K_{II} = \frac{P\sqrt{\pi a}}{wt} f_{II}\left(\frac{a}{w}\right) \quad (2)$$

where  $P$  is the applied load,  $w$  is the specimen length,  $t$  is the specimen thickness,  $a$  is the crack length, and  $f_I(a/w)$  and  $f_{II}(a/w)$  are the shaped functions for opening and shear modes, respectively.

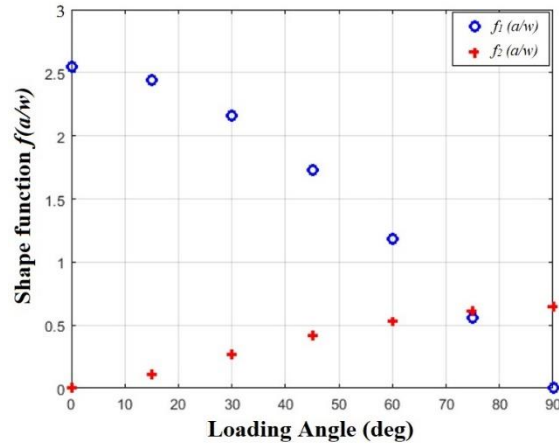


**Figure 8.** Shape functions of Arcan samples under different loading angles.

## RESULTS AND DISCUSSION

The results of tensile tests in longitudinal and transvers directions of SMC plates are shown in Fig. 9. The modulus of elasticity and yield strength of each tensile sample were determined as the slope of the elastic region and the intersection of a 0.2% strain offset of this slope with the stress-strain curve, respectively. As shown in Figure 9a, the experiments in longitudinal direction revealed an average ultimate strength of 7.9 MPa as the longitudinal tensile strength of the SMC plates. The value of elastic modulus was approximately 3.11 GPa for the same samples. Similarly, as shown in Figure 9b, the three repetitions of tensile experiments in the transverse direction revealed an average ultimate strength of 5.41 MPa as the transverse tensile strength of the SMC plates. The value of elastic modulus in transverse direction was calculated as 3.33 GPa. Therefore, the mechanical strength of SMC plates is on average 46.03% higher in longitudinal direction than

in transverse direction. The results of transversely isotropic mechanical properties of SMC plates are summarized in Table 2, while the 3-axis represents the rolling direction.

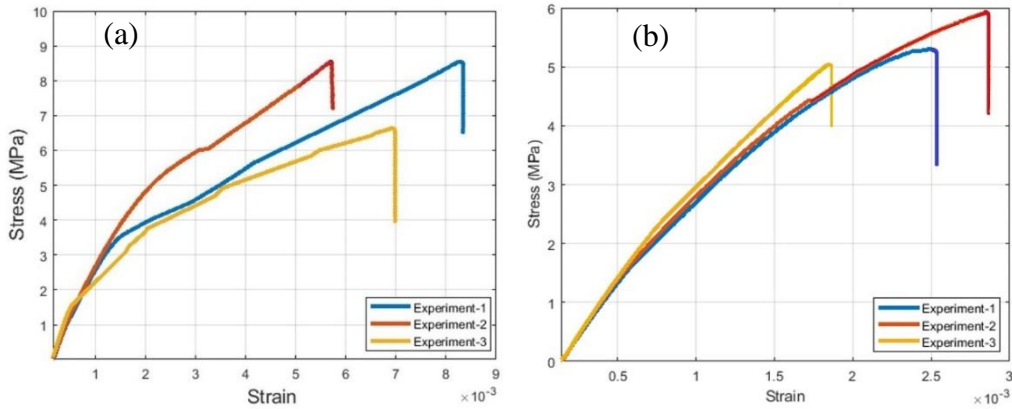


**Figure 9.** Stress-strain curves of SMC samples in; (a) longitudinal and (b) transverse directions.

**Table 2.** Transversely isotropic properties of SMC plates.

Property	Value
$E_1$ (GPa)	3.33
$E_2$ (GPa)	3.33
$E_3$ (GPa)	3.11
$G_{12}$ (GPa)	1.312
$G_{13}$ (GPa)	1.261
$G_{23}$ (GPa)	1.261
$\nu_{12}$	0.269
$\nu_{13}$	0.32
$\nu_{23}$	0.32

The results of load versus displacement curves of Arcan samples under different loading angles are represented in Figure 10. Similar to mechanical properties, the Arcan samples that have been cut in transverse direction of SMC plates represented lower fracture resistance as compared with that of longitudinally cut samples. Furthermore, the fracture load rises as the loading angle increases from pure opening ( $0^\circ$ ) to pure shearing ( $90^\circ$ ) mode. The critical load values under different modes of fracture are summarized in Table 3.

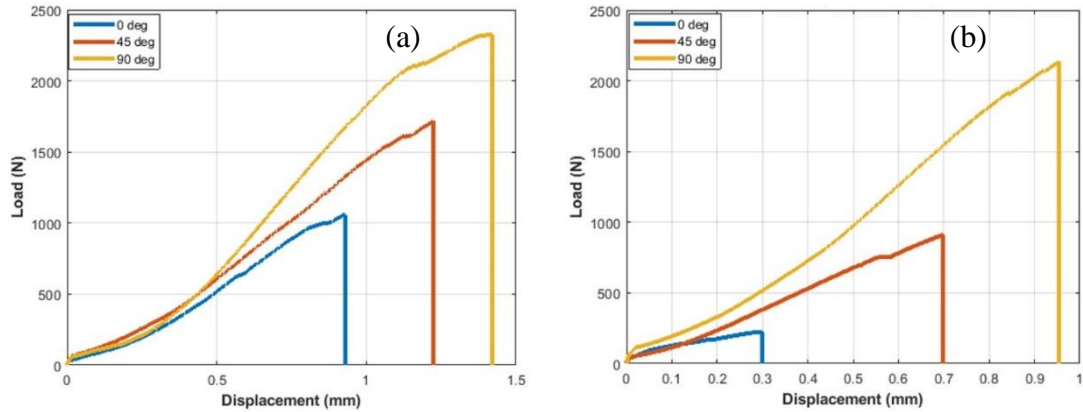


**Fig. 10.** Load vs. displacement curves of; (a) longitudinal and (b) transverse Arcan samples at different loading angles.

**Table 3.** Average fracture loading ( $P_C$  [N]) of transverse and longitudinal Arcan samples under different loading angles.

SMC direction	Loading Angle						
	0°	15°	30°	45°	60°	75°	90°
<b>Transverse</b>	223.3	423.3	639.8	910.7	1177.2	1661.0	2132.8
<b>Longitudinal</b>	1058.5	1356.3	1573.0	1716.7	1998.9	2211.7	2326.7

The critical fracture loads and shape factors have been used to calculate the critical stress intensity factors in mode-I, II and mixed-modes using Eqs. (1) and (2). The average values of transverse and longitudinal critical stress intensity factors are listed in Table 4. Accordingly, the fracture toughness for the Arcan specimen under pure mode-I loading shows an average of  $K_{IC} = 1.01$  [MPa m<sup>1/2</sup>] for transverse Arcan samples and  $K_{IC} = 4.78$  [MPa m<sup>1/2</sup>] for longitudinal Arcan samples. For pure mode-II loading, the average fracture toughness of  $K_{IIC} = 2.47$  [MPa m<sup>1/2</sup>] in transverse direction and  $K_{IIC} = 2.68$  [MPa m<sup>1/2</sup>] for longitudinal direction of SMC plates were achieved. Therefore, considering the fracture toughness under mode-I and mode-II loadings, the SMC plate possesses higher stiffness in longitudinal direction than in transverse direction of approximately 369% in mode-I and 8.5% in mode-II.

Furthermore, for plane strain conditions, the strain energy release rate can be calculated as:

$$G_I = \frac{K_I^2}{E}, \quad G_{II} = \frac{K_{II}^2}{E}, \quad \bar{E} = \frac{E}{1-\nu^2} \quad (3)$$

where  $E$  is the elastic modulus,  $\nu$  is the Poisson's ratio, and  $\bar{E}$  is the effective modulus for plane strain condition. The calculated critical energy release rates for pure mode-I, pure mode-II, and mixed-mode loading of transvers and longitudinal Arcan samples are listed in Table 5. As shown, the pure mode-I and II critical strain energy release rate of transverse SMC specimens were calculated as 250.3 and 1502.2 J/m<sup>2</sup>, respectively. In contrast, for the longitudinal Arcan samples the critical energy release rate values have been obtained as 6684.5 and 2107.3 J/m<sup>2</sup>, respectively. In general, the longitudinal Arcan samples exhibited higher fracture toughness and resistance against crack growth under all modes of loadings than that of transverse samples. This phenomenon is related to the fracture mechanisms dominated in longitudinal and transverse directions of the SMC plates. In the longitudinal direction, the main mechanisms could be the fiber breakage, pull-out and debonding from the matrix since the orientation of the fibers are mainly along the rolling direction of the plates. However, in transverse direction, crack initiation and growth at the interface of the fibers and the matrix seem to be the main fracture mechanism while fiber pull-out and debonding also exist (Mohammadzadeh *et al.*, 2019) These findings highlight the importance of consideration of rolling order of SMC plate during the production process in engineering calculations as the subsequent molding processes have little to no effect on orientation of the chopped fibers in the composite panels.

**Table 4.** Critical stress intensity factor ( $K_C$  [MPa m<sup>1/2</sup>]) of transverse and longitudinal Arcan samples under different loading angles.

SMC direction	Fracture toughness	Loading Angle						
		0°	15°	30°	45°	60°	75°	90°
Transverse	$K_{IC}$	1.01	1.83	2.45	2.79	2.47	1.65	-
	$K_{IIC}$	-	0.08	0.31	0.68	1.12	1.81	2.47
Longitudinal	$K_{IC}$	4.78	5.85	6.0	5.26	4.20	2.19	-
	$K_{IIC}$	-	0.26	0.76	1.27	1.89	2.40	2.68

**Table 5.** Critical strain energy release rate ( $G_C$  [J/m<sup>2</sup>]) of transverse and longitudinal Arcan samples under different loading angles.

SMC direction	Energy release rate	Loading Angle						
		0°	15°	30°	45°	60°	75°	90°
Transverse	$G_{IC}$	250.3	821.0	1471.8	1918.2	1504.1	667.2	-
	$G_{IIC}$	-	1.7	23.8	112.6	307.3	808.4	1504.1
	$G_T$	250.3	822.6	1495.6	2030.8	1811.4	1475.6	1504.1
Longitudinal	$G_{IC}$	6684.5	10030.0	10598.0	8103.8	5157.8	1408.2	-
	$G_{IIC}$	-	20.2	168.8	470.7	1043.0	1688.3	2107.3
	$G_T$	6684.5	10050.2	10736.8	8574.5	6200.8	3096.5	2107.3

The total strain energy release rate was calculated as  $G_T = G_{IC} + G_{IIC}$

## CONCLUSION

In this work, the commercially available chopped glass-fiber reinforced polyester SMC have been subjected to a set of uniaxial tensile and mixed-mode fracture experiments, along and perpendicular to the rolling direction. The results of these experiments were employed as input data in a finite element model based on the concept of linear elastic fracture mechanics (LEFM) and maximum tangential stress criterion to determine the fracture toughness and critical strain energy release rate of material under mixed-mode loading conditions. The main findings of this study are summarized as follows:

1. Although, the reinforcing material were in the form of strands of glass fiber, SMC specimens exhibited lower mechanical properties and fracture toughness in transverse direction that the rolling direction of SMC plates under all modes of loadings. On the other hand, the mechanical strength of SMC plates is on average 46.03% higher in longitudinal direction than in transverse direction.

2. The fracture tests revealed the fracture toughness of Arcan specimen under pure mode-I loading as an average of 1.01 [MPa m<sup>1/2</sup>] for transverse and 4.78 [MPa m<sup>1/2</sup>] for longitudinal Arcan samples, respectively. For pure mode-II loading, the average fracture toughness of 2.47 [MPa m<sup>1/2</sup>] in transverse and 2.68 [MPa m<sup>1/2</sup>] in longitudinal directions of SMC plates were achieved, respectively. Therefore, considering the fracture toughness under mode-I and mode-II loadings, the SMC plate possesses higher stiffness in longitudinal direction than in transverse direction of approximately 369% in mode-I and 8.5% in mode-II.

3. In pure mode-I and II loadings, the critical strain energy release rates of transverse SMC specimens were calculated as  $G_{IC} = 250.3$  and  $G_{IIC} = 1502.2$  J/m<sup>2</sup>, respectively. In contrast, for the longitudinal Arcan samples the critical energy release rate values have been obtained as  $G_{IC} = 6684.5$  and  $G_{IIC} = 2107.3$  J/m<sup>2</sup> for pure mode-I and II loadings, respectively. In general, the longitudinal Arcan samples exhibited higher fracture toughness and resistance against crack growth under all modes of loadings than that of transverse samples.

### ACKNOWLEDGEMENT

The authors of this study would like to thank Milen Tech and Tetraktis Composite Company for supplying SMC plates. This research received no specific grant from funding agencies in the public, commercial, or nonprofit sectors. The authors declare that there are no competing financial and/or non-financial interests that could undermine, or perceived to undermine, the objectivity, integrity and value of this article.

## REFERENCES

- Abadi, R. H., Torun, A. R., Fard, A. M. Z., & Choupani, N. 2020.** Fracture characteristics of mixed-mode toughness of dissimilar adherends (cohesive and interfacial fracture). *Journal of Adhesion Science and Technology*, 34(6), 599-615.
- Aliha, M. R. M., & Mousavi, S. S. 2020.** Sub-sized short bend beam configuration for the study of mixed-mode fracture. *Engineering Fracture Mechanics*, 225, 106830.
- Aramide, F. O., Atanda, P. O., & Olorunniwo, O. O. 2012.** Mechanical properties of a polyester fibre glass composite. *International Journal of Composite Materials*, 2(6), 147-151.
- Choupani, N. 2008.** Experimental and numerical investigation of the mixed-mode delamination in Arcan laminated specimens. *Materials Science and Engineering A*, 478: 229-242.
- Çakmakkaya, M., Kunt, M. & Terzi, O. 2019.** Investigation of polymer matrix composites in automotive consoles. *International Journal of Automotive Science And Technology*, 3 (3), 51-56.
- Ever J. Barbero 2017.** Introduction to composite materials design. 3rd edition, CRC Press.
- Ganesan, R. 2008.** 5 - Experimental characterization of interlaminar shear strength. *Delamination Behaviour of Composites*, 117-137.
- Gupta, U.S., Tiwari, S., Namdeo, R., Chaturvedi S. 2021.** Mechanical behavior of banana reinforced epoxy composite by finite element method. *Journal of Engineering Research*, DOI: 10.36909/jer.ICIPPSD.15515.
- Kelly, J., Cyr, E., & Mohammadi, M. 2018.** Finite element analysis and experimental characterisation of SMC composite car hood specimens under complex loadings. *Journal of Composites Science*, 2(3), 53.
- Lau, K. T., Hung, P. Y., Zhu, M. H., & Hui, D. 2018.** Properties of natural fibre composites for structural engineering applications. *Composites Part B: Engineering*, 136, 222-233.
- Madduru, P.R., William, A.A.S., Prashanth, M.M., Kumar, S.N.S., Ramkumar, K.D., Arivazhagan, N., Narayanan, S. 2014.** Assessment of Mechanical Properties of AISI 4140 and AISI 316 Dissimilar Weldments. *Procedia Engineering*, 75: 29-33.
- Mallick, P. K. 2012.** Failure of polymer matrix composites (PMCs) in automotive and transportation applications. In *Failure Mechanisms in Polymer Matrix Composites* (pp. 368-392). Woodhead Publishing.
- Martulli, L. M., Muyshondt, L., Kerschbaum, M., Pimenta, S., Lomov, S. V., & Swolfs, Y. 2019.** Carbon fibre sheet moulding compounds with high in-mould flow: Linking morphology to tensile and compressive properties. *Composites Part A: Applied Science and Manufacturing*, 126, 105600.
- Mohammadizadeh, M., Imeri A., Fidan, I., Elkelany, M. 2019.** 3D printed fiber reinforced polymer composites - Structural analysis. *Composites Part B*, 175: 107112.
- Nony-Davadie, C., Peltier, L., Chemisky, Y., Surowiec, B., & Meraghni, F. 2019.** Mechanical characterization of anisotropy on a carbon fiber sheet molding compound composite under quasi-static and fatigue loading. *Journal of Composite Materials*, 53(11), 1437-1457.
- Pfeiffer, F., Wriggers, P. 2012.** Lecture notes in applied and computational mechanics. *Fracture Mechanics*, 1st edition, Springer Netherlands.
- Todor, M. P., Bulei, C., & Kiss, I. 2018.** Composite materials manufacturing using textile inserts with natural origins fibres. In *IOP Conference Series: Materials Science and Engineering* (Vol. 393, No. 1, p. 012088). IOP Publishing.